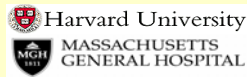


# New high resolution headmodel for accurate electromagnetic field computation

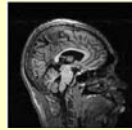


L. M. Angelone<sup>1,2</sup>, S. Tulloch<sup>3</sup>, G. Wiggins<sup>1</sup>, S. Iwaki<sup>1</sup>, N. Makris<sup>3</sup>, G. Bonmassar<sup>1</sup>



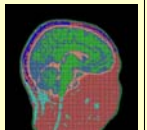
<sup>1</sup>Athinoula A. Martinos Center for Biomedical Imaging, Massachusetts General Hospital, Charlestown, MA, United States - <sup>2</sup>Biomedical Engineering Department, Tufts University, Medford, MA, United States

<sup>3</sup>Center for Morphometric Analysis, Massachusetts General Hospital, Charlestown, MA, United States



## RATIONALE: Why?

Realistic head models are commonly used for the computation of the electromagnetic fields, which are mostly used for RF coil design and safety studies [1-4]. The resolution of the head model generally affects the accuracy of the electromagnetic field computation.



## METHODS: How?

One high-resolution head model (1x1x1mm<sup>3</sup>) was manually segmented from the anatomical MRI data of an adult male subject. The subject anatomical MRI was performed with a quadrature birdcage transmit/receive head coil on our 1.5T scanner (General Electric, Milwaukee, WI, USA). Three whole-head scans were collected with a T1-weighted 3D-SPGR sequence (TR/TE=24/8ms) with 124 slices, 1.3mm thick (matrix size 256x192, FOV 256mm). The individual images were motion-corrected and averaged to increase gray/white matter contrast-to-noise ratio using MEDx software (Sensor Systems, Inc., Sterling, VA, USA). Twenty six different types of tissue were manually segmented from the MRI image.

The head model was used for evaluation of RF power distribution in MRI using FDTD algorithm (XFDTD, REMCOM Co., State College, USA). Each cell of the head model was isotropic and of dimensions 1x1x1mm<sup>3</sup>. The physical properties of tissue were selected according to the literature [6] (Table 1.) The total number of Yee cells [7] for the head models was 4642730. The total volume considered including the free space around the model was 296x390x351mm<sup>3</sup>. Simulation studies with the head model were conducted with birdcage coil [4] at 128MHz-3T and 300MHz-7T.

Fig. 1

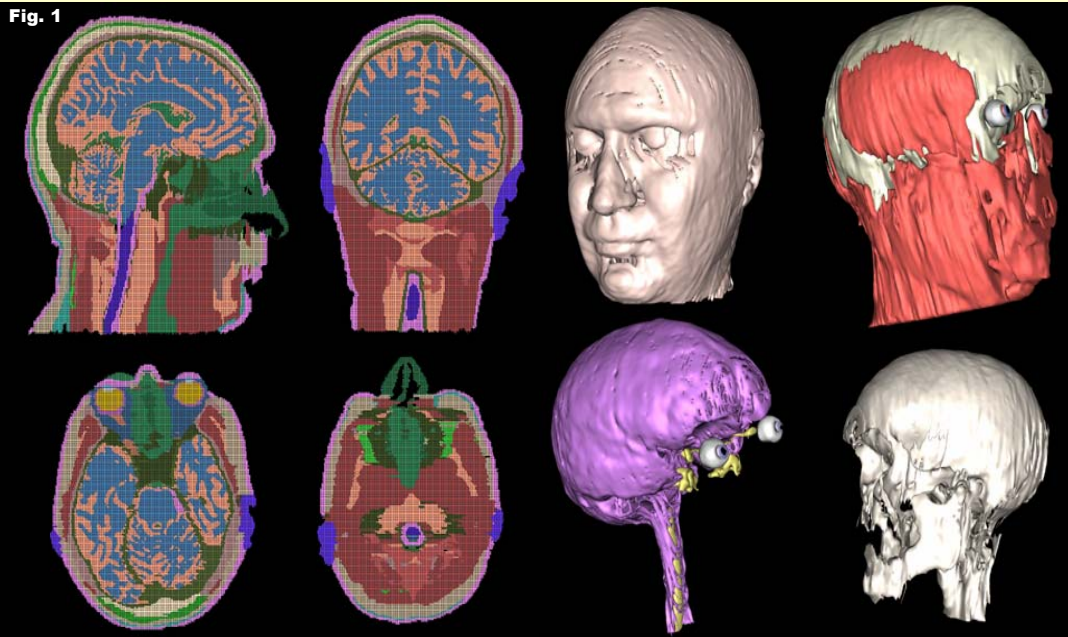


Table 1

TISSUES	Density (Kg/m <sup>3</sup> )	Weight (g)	300MHz	
			$\sigma$ (S/m)	$\epsilon_r$
CSF*	1010	20.05	2.22	72.73
Grey Matter*	1040	512.82	0.69	60.02
White Matter*	1040	916.70	0.41	43.77
Adipose*	920	36.45	0.08	11.74
Air*	1	0.08	0.00	1.00
Bone*	1850	316.15	0.22	23.16
Aqueous-Humor*	1000	0.16	1.00	100.00
Conn-Tissue (Cartilage + blood**)	1096	31.44	0.63	48.66
Cornea*	1000	0.07	1.15	61.37
CSF_SA*	1010	17.41	2.22	72.73
Diploe*	970	133.00	0.17	12.13
Dura*	1850	381.01	0.80	47.96
Ear*	1100	44.31	0.55	46.77
Epidermis*	1010	389.67	0.63	52.00
Inner-Table*	1850	477.94	0.22	23.16
Lens (Cartilage**)	1100	0.46	0.55	46.77
Muscle*	1040	1133.83	0.69	58.97
Nasal-Structures*	1100	61.24	0.55	46.77
Nerve*	1040	6.37	0.42	36.91
Orbital-Fat*	920	38.77	0.08	11.74
Outer-Table*	1850	121.57	0.22	23.16
Subcutaneous Tissue (Cartilage+ Blood**)	1096	47.02	0.63	42.23
R/C/S (Retina/Cornea/Sclera)*	1170	6.74	0.98	58.90
SC-Fat/Muscle**	980	374.52	0.38	35.36
Soft-Tissue (Avg. Muscle - Conn.Tiss. Bone Fat **)	1226.5	164.11	0.40	35.63
Spinal-Cord*	1040	7.20	0.42	36.91
Teeth*	1850	39.27	0.22	23.16
Tongue*	1040	19.74	0.74	59.00
Vitreous-Humour*	1000	8.26	1.51	69.00

\* Tissues properties as in FCC [6]  
\*\* Tissue properties obtained as average

## RESULTS: What?

The simulated B-field showed the typical dielectric resonance at 7T [8]. The B-field distribution was in general much closer to the real case (Fig. 2 A) since it showed positive peaks in the ventricles (Fig. 2 B) whereas the 8-tissues head model with the same resolution (Fig. 2 C) showed a negative peak in the midbrain region. The peak of SAR was in the Nasal structures, near a source [3]. Local SAR increases could be partly enhanced due to staircasing effects [9]. However the high number of cells per wavelength (2000 cells at 128 MHz, 1000 cells at 300 MHz) should reduce the staircase error to less than 1dB [10]. Furthermore, the position of the peak SAR values were consistent with the literature [3, 11]. Similar results were obtained modeling an end-cap TEM coil (D).

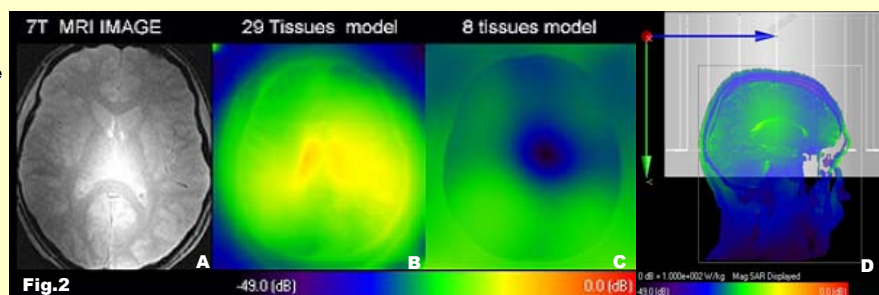


FIGURE (A) MRI image showing the typical dielectric resonance at 7T localized in the center. (B & C) B1 field distribution calculated with the new head model (B) compared with 8 tissues head model (C) using birdcage coil at 7T. (D) SAR distribution with end-cap TEM at 300MHz

## CONCLUSIONS

We present a new high resolution head model that can be a usefully utilized for electromagnetic fields computation. Results obtained are in agreement with the literature and outperform the accuracy in estimating the distribution of the B1 field of a model with same resolution but with a lower number of tissues.

## ACKNOWLEDGEMENTS

We thank David Carpenter of REMCOM, George Papadimitriou, James Howard, Andreas Potthast, Chris Wiggins, Larry Wald, and Bruce Rosen. All at the Athinoula A. Martinos Center for Biomedical Imaging. Study supported by NIH grants R01 EB002459-01, P41 RR014075, and the MIND Institute.

## REFERENCES

1. Collins, C.M., et al., Magn Reson Med, 1998. 40(6): p. 847-56. 2. Jin, J., et al., Magn Reson Med, 1997. 3. Ibrahim, T.S., et al., Phys Med Biol, 2001. 4. Angelone, L.M., et al., Bioelectromagnetics, 2004. 5. Dale, A.M., et al., Neuroimage, 1999. 6. FCC, <http://www.fcc.gov/fcc-bin/dielec.sh> 7. Yee, K.S., IEEE Transactions on Antennas and Propagation, 1966. 8. Vaughan, J.T., et al., Magn Reson Med, 2001. 9. Gangelaris, A.C., et al., IEEE Transactions on Antennas and Propagation, 1991. 39: p. 1518-1525. 10. Holland, R., IEEE Trans on Electromagnetics Compatibility, 1993. 11. Chou, C.K., et al., Bioelectromagnetics, 1996.

## CONTACT INFO

Leonardo M. Angelone, Athinoula A. Martinos Center for Biomedical Imaging, Bldg. 149, 13<sup>th</sup> Street, Charlestown, MA angelone@mnr.mgh.harvard.edu